J. Phys. B: Atom. Molec. Phys., Vol. 12, No. 7, 1979. Printed in Great Britain

LETTER TO THE EDITOR

Measured cross sections for ionisation of C^{3+}, N^{4+} and O^{5+} ions with contribution due to excitation-autoionisation

D H Crandall†, R A Phaneuf†, B E Hasselquist† and D C Gregory‡§

†Oak Ridge National Laboratory, Oak Ridge, Tennessee 37830, USA

‡Joint Institute for Laboratory Astrophysics, The University of Colorado and National Bureau of Standards, Boulder, Colorado 80309, USA

Received 22 January 1979

Abstract. Measured cross sections for electron impact ionisation of Li-like ions of C^{3+}, N^{4+} and O^{5+} are reported for energies from threshold to 1500 eV. For electron energies from near threshold through the first peak in the cross sections, the measured values are in reasonable agreement with Coulomb–Born calculations. However, in each case an abrupt increase in the measured ionisation cross section is observed at the electron energy associated with excitation of an inner-shell electron, a process which has not been included in the theories. The $1s^22s \rightarrow 1s2s2l$ excitation followed by autoionisation is shown to give an abrupt and significant contribution to the total ionisation cross section. Further, the relative contribution of the excitation-autoionisation process increases with increasing ionic (or nuclear) charge for the three cases tested along the Li isoelectronic sequence.

A previous paper by Crandall *et al* (1978, hereafter referred to as I) reported the measured cross sections for electron impact ionisation of C^{3+} and N^{4+} for electron energies up to 500 eV. At the highest measured energies, those cross sections exceeded the direct Coulomb–Born calculation by Moores (1978) and the scaled Coulomb–Born estimate of Golden and Sampson (1977) based on the Coulomb–Born predictions for hydrogenic ions of infinite charge. In I and in Moores (1978), the possibility of excitation-autoionisation contributing to the cross sections was postulated as the source of the discrepancy between the experiment and the theories. After minor apparatus modifications, the experiments have been repeated with improved statistical precision, a finer energy grid, and an extension of the energy range to 1500 eV. In addition, measurements on the next member of the isoelectronic sequence, O^{5+}, have been completed. The contribution of excitation-autoionisation to the total ionisation cross section is confirmed, and the relative importance of this process is observed to increase with increasing ionic charge along the Li isoelectronic sequence.

Details of the electron–ion crossed-beams apparatus and the associated difficulties and diagnostics are described in I. Ions of energy $10\,\mathrm{keV}\times q$ (where q is the ionic charge) are crossed at right angles by a variable energy electron beam. After the beam crossing point, those ions which have increased their charge by one unit are separated from the incident ions by two stages of electrostatic analysis. Gating of beams and detectors separates the ionisation signal due to the beams' interaction from that originating with background gas and other processes. The only modification of the apparatus from that described in I is the addition of a second stage of electrostatic

§ Present address: Brookhaven National Laboratory, Upton, LI, New York, 11973, USA.

analysis for the primary ion beam in the post-scattering region. Now both the primary beam and the component ionised to the next higher charge state pass through two stages of electrostatic analysis. This additional deflection of the primary ion beam reduced the background of photons produced at the collector of the primary beam which, after reflection, were observed by the channel electron multiplier used to detect the signal of ions of increased charge. The improved signal-to-noise ratio allowed about a factor of three higher statistical precision in the ionisation cross section measurements. Other minor changes external to the ultra-high vacuum collision chamber allowed extension of the electron energy to 1500 eV.

Figures 1, 2, and 3 and table 1 present the measured cross sections for electron impact ionisation of C^{3+}, N^{4+} and O^{5+} and compare these with available theory. The experimental cross section values are independently absolute. This derives from accurate determinations of incident ion and electron beam fluxes, the beam-overlap form factor at the crossing point, and the overall efficiency for detection of the signal ions which have increased their charge by one unit. The total absolute uncertainty for the present measurements (see table 1) is about a factor of two better than for the previous data (I) due to the improved counting statistics and to significantly improved confidence in the efficiency of collecting and detecting signal ions, which for the

Table 1. Most of the actual data values plotted in figures 1–3 are tabulated. The uncertainties listed are 90% confidence level counting statistics. Additional systematic uncertainty of ±6% for C^{3+} and N^{4+} and of ±10% for O^{5+} should be added in quadrature with individual statistical uncertainty to obtain good confidence absolute uncertainty.

X / E/E_{th}	C^{3+} (64·45 eV) σ_{34} (10^{-18} cm^2)	N^{4+} (97·86 eV) σ_{45} (10^{-18} cm^2)	O^{5+} (138·1 eV) σ_{56} (10^{-18} cm^2)
1·09	0·46±0·20	0·28±0·04	
1·17	1·07±0·20	0·56±0·08	0·31±0·18
1·25	1·20±0·19	0·74±0·04	
1·40	1·43±0·17	0·93±0·04	0·45±0·17
1·70		1·21±0·05	0·70±0·12
2·00		1·27±0·05	
2·2	2·51±0·11		0·82±0·15
2·5		1·45±0·04	
3·0		1·47±0·04	0·75±0·10
3·6	2·59±0·04	1·40±0·05	0·67±0·05
4·0	2·37±0·05	1·32±0·03	0·76±0·10
4·2	2·40±0·04	1·33±0·04	0·84±0·10
4·4	2·33±0·04	1·41±0·04	
4·6	2·37±0·03	1·42±0·04	0·89±0·08
4·8	2·47±0·03	1·44±0·04	
5·0	2·49±0·04	1·46±0·04	0·88±0·12
5·25	2·39±0·04	1·42±0·04	
5·6		1·41±0·04	0·88±0·14
6·0	2·41±0·07	1·40±0·04	
7·0	2·25±0·06	1·35±0·04	0·74±0·36
8·0	2·10±0·11	1·30±0·02	0·70±0·14
10·0	2·00±0·07	1·22±0·03	0·48±0·10
12·0	1·92±0·08	1·16±0·04	
15·0	1·78±0·04	1·05±0·05	
18·3	1·47±0·08		
22·9	1·37±0·06		

modified apparatus is determined to be $(98 \pm 3)\%$. Table 1 contains only those cross section values measured in the present experiment, though the previously measured values (I) agree well and could have been incorporated into the table and figures.

For C^{3+} (figure 1) the Coulomb–Born calculated cross sections are about 25% higher than present data at the peak of direct ionisation, which occurs at an energy about 2·8 times the 64·5 eV threshold for ionisation. The Coulomb–Born results then decrease smoothly (the results of Moores (1978) actually extend smoothly up to 590 eV but have been curtailed at 250 eV on figure 1 in order to show other results). The experimental values increase again abruptly by about 10% at 300 ($\pm$5) eV. The energy of this feature coincides with the energy for excitation $1s^22s \rightarrow 1s2s2l$ (where l = s or p). There are four states of configuration $1s2s2l$, all within 5 eV of 300 eV, which can be excited by electron impact excitation of one 1s electron; they are $(1s2s^2)^2S$ at 294·0 eV, $(1s2s2p)^4P^o$ at 294·2 eV, and two states of configuration $(1s2s2p)^2P$ at 299·8 and 303·9 eV. These energies are taken from Magee *et al* (1977), and for the ^4P level there is good agreement with the tabulated spectroscopic values given by Bashkin and Stoner (1975). In fact the collision strengths for electron impact excitation of these four levels of C^{3+} are tabulated in the report of Magee *et al* (1977) as calculated by J B Mann in a Coulomb–Born with exchange approximation. For comparison, these calculated collision strengths have been converted to cross sections and added to the scaled Coulomb–Born result on figure 1. The comparison of these summed excitation cross sections with the presently observed increase in ionisation cross sections is remarkably good, being about $0{\cdot}3 \times 10^{-18}$ cm^2 in both cases at 315 eV (near threshold for the excitation process).

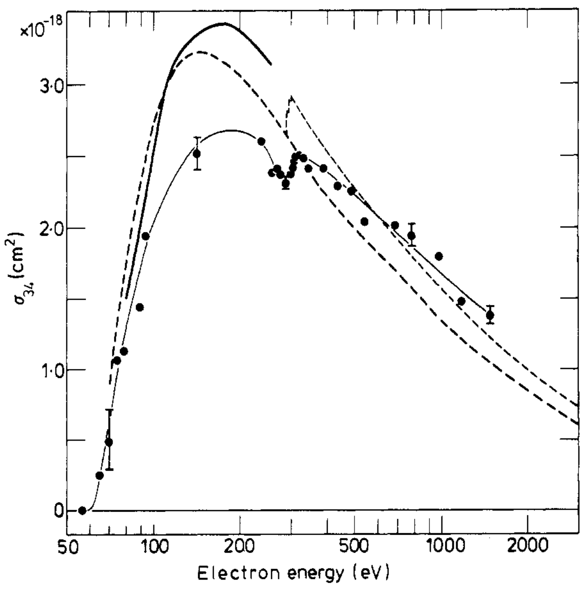

Figure 1. Cross section for electron impact ionisation of C^{3+}. The connected full circles are present data; the broken curve is scaled Coulomb–Born of Golden and Sampson (1977); the full bold curve is Coulomb–Born by Moores (1978); the short-dashed curve is the summed excitation cross sections for $1s^22s \rightarrow 1s2s2l$ given by Magee *et al* (1977) added to the scaled Coulomb–Born beginning at the 294 eV excitation threshold. The error bars shown are typical statistical uncertainties at 90% confidence level (see table 1).

Several assumptions are required in comparing the calculated excitation cross sections with the increase in the measured ionisation cross section. First, the shape of the excitation thresholds is assumed to be a step function for each state as predicted by theory, and the experimentally observed slope is attributed to a convolution of experimental spread (about ±5 eV at 300 eV) with the excitation cross sections to the various states which have a progression of threshold energies extending over several eV. Second, in the experiment the inner-shell excited ions are all assumed to decay by autoionisation before they are separated according to charge so that the observed increase in ionisation cross section should indeed correspond to the inner-shell excitation cross sections. This second assumption is expected to be valid, even for the metastable $(1s2s2p)^4P^o$ state, which should decay by autoionisation easily within the roughly 0·3 μs flight time from collision centre to ion dispersion region (see Livingston and Berry 1978). The calculated contribution of the excitation to the ^4P level is about one quarter of the total excitation at threshold, but at higher energies the excitation to this level becomes negligible because of the generally faster decrease of such spin-forbidden excitations as energy increases. Third, the higher n level excitations—for example $1s^22s \rightarrow 1s2s3l$—have not been included in the sum of the calculated excitation cross sections. This omission may account for the discrepancy between the high energy trends of the measured and calculated cross sections apparent on figure 1.

No attempt is made here to compare the measured cross sections with less definitive calculated values from classical, semi-empirical, or ECIP-type models. However, such comparisons are given in I for the direct ionisation process.

Figure 2 shows comparison of present data with Coulomb–Born calculations for the N^{4+} case. Here the agreement between these theories and the experiment for energies from the 97·8 eV ionisation threshold to 400 eV is excellent. The observed increase in

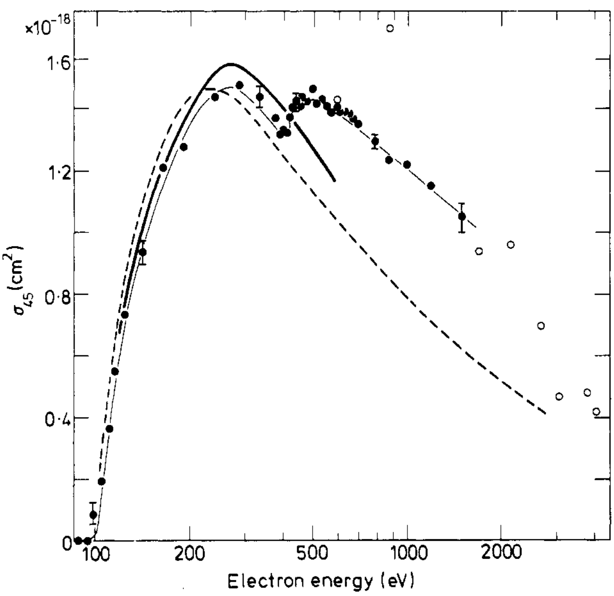

Figure 2. Cross section for electron impact ionisation of N^{4+}. The connected full circles are present data; open circles are data of Donets and Ovsyannikov (1977); broken curve is scaled Coulomb–Born of Golden and Sampson (1977); full bold curve is Coulomb–Born by Moores (1978).

ionisation cross section at 420 (±5) eV is qualitatively identical with the C^{3+} case and is attributed to the same process. In the present N^{4+} case the increase due to excitation-autoionisation is about 14% and is larger than for C^{3+}.

Theoretical energies and excitation cross sections for $1s^22s \rightarrow 1s2s2l$ transitions in N^{4+} have been obtained from R J W Henry (1979, private communication) who carried out the calculations in a six-state close-coupling approximation with configuration interaction on each of the states. The threshold energies he obtains are 413 eV for $(1s2s^2)^2S$, 416 eV for $(1s2s2p)^4P$, and 423 eV and 429 eV for the two strongly mixed $(1s2s2p)^2P$ states. The sum of the theoretical excitation cross sections is $1{\cdot}27\times10^{-19}$ cm^2 at 456 eV and $0{\cdot}83\times10^{-19}$ cm^2 at 1361 eV. From the present ionisation data the increase in ionisation attributed to excitation of these levels is about $1{\cdot}6\times10^{-19}$ cm^2 at 456 eV. This value is 25% higher than the close-coupling result, but the agreement is within the uncertainty associated with estimating the excitation cross section from the ionisation data. As for the C^{3+} case, the high energy trend of the N^{4+} ionisation cross section disagrees with the scaled Coulomb–Born even with the $1s^22s \rightarrow 1s2s2l$ excitations added, but excitations of higher n levels have not been included.

Donets and Ovsyannikov (1977) obtained their high energy data by modelling the ionisation produced and observed after turning on the high current, nearly monoenergetic, electron source inside their electron beam ion source (EBIS). Since the cross sections obtained from the EBIS are modelling dependent, they are not believed to be as definitive as present measurements, but, except for the single point at 890 eV, the results are quite consistent with the present N^{4+} data.

The present results for ionisation of O^{5+} are compared to the scaled Coulomb–Born estimate in figure 3. Again the experiment and theory are in excellent agreement from the 138 eV threshold for ionisation up to 500 eV. The accentuated small feature in the scaled Coulomb–Born theory beginning about 800 eV illustrates onset of direct ionisation of an inner-shell electron. For these O^{5+} measurements, the abrupt increase in ionisation cross section is at 530 (±20) eV, and the increase of about 30% is still larger than in the N^{4+} case. With the assumption that the presence of the outer 2s electron does not affect the energy interval appreciably, the estimated $1s^22s \rightarrow 1s2s2l$ excitation energies would be about the same as the $O^{6+}(1s^2 \rightarrow 1s2l)$ excitations which are tabulated (Bashkin and Stoner 1975) to be between 561 and 547 eV—in reasonable agreement with the onset energy of the increase in O^{5+} ionisation.

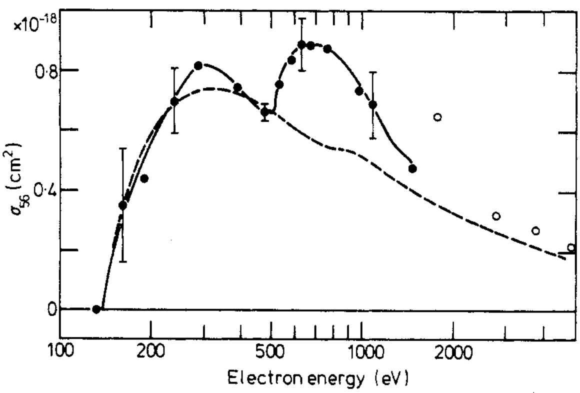

Figure 3. Cross section for electron impact ionisation of O^{5+}. The connected full circles are present data; open circles are data of Donets and Ovsyannikov (1977); broken curve is scaled Coulomb–Born of Golden and Sampson (1977).

There is a minor qualitative difference between the O^{5+} case and either of the C^{3+} and N^{4+} cases in that the high energy trend of the O^{5+} data shows a rapid convergence toward the direct scaled Coulomb–Born result. The last three data points of the O^{5+} case, which suggest this convergence, are the least reliable of all the data presented here since they are at the highest energies and weakest signal levels, where undetected systematic errors are possible. (Extensive diagnostics were performed at high energy for the N^{4+} with no systematic errors revealed, but those tests were not repeated in the more difficult O^{5+} case.) Nevertheless, the apparent convergence of the O^{5+} experimental data with the scaled Coulomb–Born calculation could be justified for this case if the excitation-autoionisation contribution proceeds dominantly through the $(1s2s2p)^4P^o$ state. Considering the calculated excitation transitions for C^{3+} (Magee *et al* 1977) and N^{4+} (R J W Henry 1979, private communication), the spin forbidden excitation of the ^4P state has the behaviour observed for the O^{5+} excitation-autoionisation contribution; that is, it falls off abruptly above threshold when compared with the spin-allowed transitions calculated to dominate the C^{3+} and N^{4+} cases.

None of the present data follow the high energy behaviour predicted by the scaled Coulomb–Born calculation. For C^{3+}, and to a lesser degree for N^{4+}, the measured cross sections decrease less rapidly than the Coulomb–Born, while for O^{5+} the experimental cross section appears to decrease more rapidly than the Coulomb–Born. Whatever the cause of these discrepancies, the present data illustrate that convergence of ionisation cross sections to the usually accepted $E^{-1}\log E$ high energy behaviour may not always occur—at least not until relatively high energies.

The observation of the excitation-autoionisation contribution to ionisation cross sections is not unique to the present data. Peart and Dolder (1968), Feeney *et al* (1972), and Dolder and Peart (1976) present data for the alkali-like ions Mg^+, Ca^+, Sr^+, Ba^+ and observe up to a six-fold increase (Ba^+ case) in ionisation due to excitation-autoionisation. In their data the process is attributed dominantly to excitation transitions such as $3p^6 4s \rightarrow 3p^5 3d4s$ (Ca^+ case) which then autoionise.

An important feature of the present data is the increase of the excitation-autoionisation contribution with increasing charge along an isoelectronic sequence. As a simple comparison the ratios of the measured cross sections at the second (excitation-autoionisation) peak to those at the first (direct ionisation) peak are plotted on figure 4

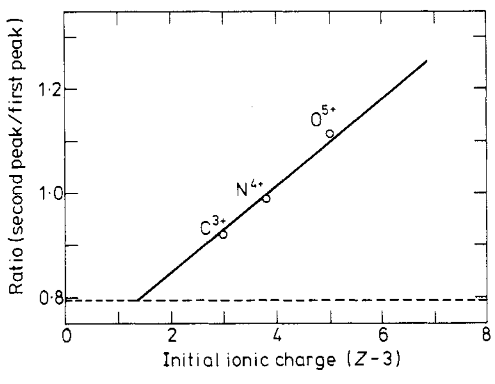

Figure 4. Ratio of the cross section value at the second (excitation-autoionisation) peak to the cross section value at the first (direct) peak as a function of initial ionic charge for present measured values of C^{3+}, N^{4+} and O^{5+}. The broken-line value is the average value of this ratio from the scaled Coulomb–Born ionisation calculations which predict no second peak.

against the initial ionic charge q. The broken line value on figure 4 is the average ratio predicted by the scaled Coulomb–Born estimates in which there are no second peaks, i.e. the value of the theoretical direct ionisation cross section at the energy location of the observed excitation-ionisation peak is divided by the theoretical value at the peak of direct ionisation. Within the accuracy and extent of the present data, the relative contribution of the excitation-autoionisation increases linearly with ionic charge as shown in figure 4. Bely (1968) has presented a scaled Coulomb–Born calculation for Na-like ions which predicts a significant contribution to ionisation by the excitation of 2s and 2p electrons followed by autoionisation. As in the present Li-like case, the predicted relative contribution of excitation-autoionisation increases with ionic charge for the Na-like sequence, although the relative increase is not linear but diminishes for higher charge states. It is noted that Bely's predictions for the Mg^+ case are not born out by the observations of Martin *et al* (1968). A further caution, appropriate to estimating the effect of excitation-autoionisation for highly charged ions, is that the radiative lifetimes of the excited ions eventually will become comparable to autoionisation lifetimes so that the ions may radiate rather than autoionise. Hahn (1978) has included this fluorescence yield effect with distorted-wave calculations of the relative importance of direct and excitation-autoionisation contributions to ionisation for a few highly charged ions (no Li-like ions included). He finds at least one case, Mo^{24+}, where excitation-autoionisation is larger than direct ionisation even after radiative decay is considered.

For C^{3+} and N^{4+} the ionisation rates derived from measured cross sections and presented in I will not be changed for the present data except at very high electron temperatures. However, the trend in the present data implies that, for higher charge states (e.g. Ar^{15+} or Fe^{23+}), excitation-autoionisation could have a significant effect on ionisation rates of highly charged Li-like ions in high temperature plasmas of fusion and astrophysics where such ions occur. The possibility of excitation-autoionisation increasing ionisation rates has been previously recognised in astrophysics—see Goldberg *et al* (1965) and Burgess *et al* (1977), but more definitive work on this process is needed. Of course, in plasmas the coupling of excitation, ionisation, autoionisation, and recombination must be fully accounted for (see Jacobs and Davis 1978), so that accurate estimates of the basic processes are only a beginning.

The function of the present paper is to present accurate experimental data for some test cases and to illustrate the progressive importance of the excitation-autoionisation process for highly charged ions. The examples of the C^{3+} and N^{4+} data in comparison with available theory illustrate that the theoretical capability to address the issue is available.

We gratefully acknowledge discussion of theoretical excitation results with R J W Henry and J B Mann and discussion of the experiment with G H Dunn and C F Barnett. Technical assistance was provided by J W Hale and F W Meyer. This work has been supported by the Divisions Basic Energy Sciences and Magnetic Fusion Energy of the US Department of Energy under Contract W-7405-eng-26 with Union Carbide Corporation.

References

Bashkin S and Stoner J O Jr 1975 *Atomic Energy Levels and Grotrian Diagrams* vol 1 (Amsterdam and Oxford: North-Holland and New York: Elsevier)

Bely O 1968 *J. Phys. B: Atom. Molec. Phys.* **1** 23–7
Burgess A, Summers H P, Cochrane D M and McWhirter R W P 1977 *Mon. Not. R. Astron. Soc.* **179** 275–92
Crandall D H, Phaneuf R A and Taylor P O 1978 *Phys. Rev.* A **18** 1911–24
Dolder K T and Peart B 1976 *Rep. Prog. Phys.* **39** 693–749
Donets E D and Ovsyannikov V P 1977 *Joint Institute of Nuclear Research, Dubna, Report No* P7-10780 (translation ORNL tr-4616 available from Tech. Info. Center, PO Box 62, Oak Ridge, TN 37830, USA)
Feeney R K, Hooper J W and Elford M T 1972 *Phys Rev.* A **6** 1469–78
Goldberg L, Dupree A K and Allen J W 1965 *Ann. Astrophys.* **28** 589–92
Golden L B and Sampson D H 1977 *J. Phys. B: Atom. Molec. Phys.* **10** 2229–37
Hahn Y 1978 *Phys. Rev.* A **18** 1029–37
Jacobs V L and Davis J 1978 *Phys. Rev.* A **18** 697–710
Livingston A E and Berry H G 1978 *Phys. Rev.* A **17** 1966–75
Magee N H Jr, Mann J B, Merts A L and Robb W D 1977 *Los Alamos Scientific Laboratory, Los Alamos, Report* LA 6691MS, pp 109–12
Martin S O, Peart B and Dolder K T 1968 *J. Phys. B: Atom. Molec. Phys.* **1** 537–42
Moores D L 1978 *J. Phys. B: Atom. Molec. Phys.* **11** L403–5
Peart B and Dolder K T 1968 *J. Phys. B: Atom. Molec. Phys.* **1** 872